Passive, Broadband, and Low-Frequency Suppression of Laser Amplitude Noise to the Shot-Noise Limit Using a Hollow-Core Fiber

Euan J. Allen, Giacomo Ferranti, Kristina R. Rusimova, Robert J.A. Francis-Jones, Maria Azini, Dylan H. Mahler, Timothy C. Ralph, Peter J. Mosley, and Jonathan C.F. Matthews

Phys. Rev. Applied **12**, 044073 — Published 31 October 2019

DOI: 10.1103/PhysRevApplied.12.044073

Passive, broadband and low-frequency suppression of laser amplitude noise to the shot-noise limit using hollow-core fibre

Euan J. Allen[*1, 2], Giacomo Ferranti[1], Kristina R. Rusimova[3], Robert J. A. Francis-Jones[3, 4], Maria Azini[3], Dylan H. Mahler[1, 5], Timothy C. Ralph[6], Peter J. Mosley[3], and Jonathan C. F. Matthews[1]

[1]*Quantum Engineering Technologies Labs, H. H. Wills Physics Laboratory and Department of Electrical & Electronic Engineering, University of Bristol, BS8 1FD, United Kingdom*

[2]*Quantum Engineering Centre for Doctoral Training, Nanoscience and Quantum Information Centre, University of Bristol, BS8 1FD, United Kingdom*

[3]*Centre for Photonics and Photonic Materials, Department of Physics, University of Bath, Bath, BA2 7AY, United Kingdom*

[4]*Now at Clarendon Laboratory, University of Oxford, Parks Road, Oxford, OX1 3PU, United Kingdom*

[5]*Now at Xanadu, 372 Richmond St W, Toronto, ON M5V 2L7, Canada*

[6]*Centre for Quantum Computation and Communication Technology, School of Mathematics and Physics, University of Queensland, Brisbane, Queensland 4072, Australia and*

*euan.allen@bristol.ac.uk

Reducing noise to the shot-noise limit is a challenge for laser development for ultra-sensitive applications in precision sensing and fundamental science. We use hollow-core fibre in a collinear balanced detection scheme to suppress 2.6 dB of amplitude noise to within 0.01 dB of the shot-noise limit, whilst simultaneously preserving the spectrum and temporal profile of picosecond laser pulses. We also provide an enhanced version of the scheme which concatenates multiple circuits to suppress over many frequencies and broad frequency ranges. We perform a first demonstration of this method and reduce total excess amplitude noise, between 2 - 6 MHz, by 85%. These demonstrations enable passive, broadband, all-guided fibre laser technology operating at the shot-noise limit.

I. INTRODUCTION

Doped fibre lasers are attractive due to their low cost, compact size and robust stable operation. However, they exhibit classical intensity noise well above the optical shot-noise limit due to stimulated spontaneous emission [1–4]. To suppress this extra noise, existing noise suppression techniques could in principle enable use of fibre lasers for ultra-sensitive applications. However, direct changes to the laser itself — such as intracavity spectral filtering [5] and optical feedback into the laser cavity [6, 7] — or external methods — such as feedback or feedforward circuits coupled to an optical modulator [8, 9] or external cavity filtering [10] — all require fast and low-noise electronics. The speed of such electronics limits the bandwidth that can be filtered, while electronic noise can be transferred back into the optical beam.

In practice, the ability of these schemes to reach the shot-noise limit can be hindered by fundamental limitations of two beams output from a beamsplitter being uncorrelated on the quantum level [11]. They can also suffer from technical issues such as non-zero time response of any feedback mechanism [12], beam-geometry and pointing issues [9], and the tradeoff when tailoring the speed or gain of the feedback mechanism to reduce noise across a large bandwidth [8–10, 12]. Removing common mode noise using balanced detection [13] is passive, however optical intensity must be equally split across the two detectors in order to remove all classical noise; this is impossible for optical transmission measurements or imaging whenever the sample introduces unknown loss prior to detection.

II. COLLINEAR-BALANCED DETECTION

Collinear balanced detection (CBD) is a passive method that requires no knowledge of beam intensity and no intensity subtraction [14]. It comprises an optical delay in a static asymmetric Mach-Zehnder interferometer (AMZI) to provide an output beam with shot-noise limited intensity fluctuation at one frequency. This has been used, with a free space delay of 8.6 m, to increase the quality of stimulated Raman microscopy measured at 17.5 MHz [14] and to suppress classical noise from a noisy fibre laser used to generate amplitude-squeezed light with intensity fluctuations below the optical shot-noise limit at $20 - 24$ MHz [15]. However, two criticisms of CBD are that existing demonstrations have used free-space delays which require the stability of optical isolation tables, and that existing CBD demonstrations suppress noise at only one frequency [16]. Here we address both points, by demonstrating a fibre optic approach — that is more robust than a free-space approach — and we introduce an iterated approach that allows suppression of noise at multiple frequencies simultaneously.

The original CBD concept is illustrated in Fig. 1 (a). A train of laser pulses are launched into one input of an AMZI, where one path inside imparts a relative time delay of $\tau = Ln/c$ (L is the length of delay medium of refractive index n) such that the pulses in the delayed

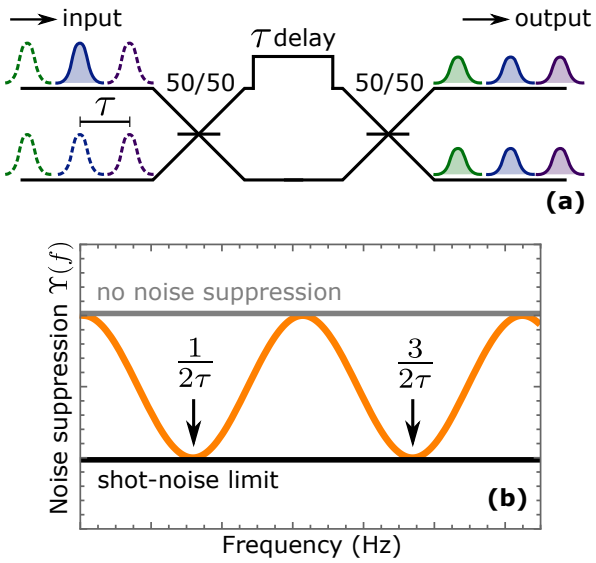

FIG. 1. (a) Collinear balanced detection setup which produces shot-noise limited light at the output of the interferometer which double the repetition rate, half the average power and a quarter of the peak power of the original pulse train. (b) Theoretical plot (Eq. 1) of classical noise suppressed by CBD over a range of noise frequencies given a single delay of τ. CBD causes complete suppression odd multiples of the frequency $f = 1/(2\tau)$ at both outputs. Colour online.

and non-delayed paths do not overlap in time when their paths re-combine at the second beamsplitter. Note that because the pulses do not optically interfere at the second beamsplitter, the AMZI requires no phase stabilisation. Output from the CBD circuit, for a given τ, are two beams that both have a classical noise suppression factor Υ, which follow a sinusoidal function (Fig. 1 (b)) that reaches the shot-noise limit at odd multiples of $f = 1/2\tau$ [14],

$$\Upsilon(f) = \frac{1}{2}\left(1 + \cos[\pi f \tau]\right), \tag{1}$$

where $\Upsilon(f) = 1$ or $\Upsilon(f) = 0$ indicates that either zero or total classical noise suppression has occurred respectively (the latter becoming shot-noise limited). To remove noise at a frequency f, a delay of length $L = c/(2nf)$ should be implemented.

The inverse relation with the suppression frequency ($\tau = 1/2f$) means the delay required for lower frequency noise suppression becomes increasingly challenging to build and maintain in free-space. For example, suppressing noise at 5 MHz requires 30 m of free-space delay. Constructing a waveguided delay long enough to suppress noise at low frequencies therefore makes CBD more practical and would allow integration of passive all-guided noise suppression with fibre lasers. Solid-core optical fibre, such as SMF-28, has the potential to filter noise at sub-kHz frequencies thanks to the availability of lengths of many kilometres — we illustrate this in the Supplementary Material with results for a 4.3 km delay that suppresses amplitude noise at 25 kHz. However, self-phase modulation and dispersion occur when laser pulses traverse solid-core fibre, which for the CBD scheme results in half of the output pulses being spectrally broadened and temporally elongated — this is undesirable when the filtered light is to be used for applications sensitive to the spectral and temporal profile of laser pulses, such as nonlinear spectroscopy, microscopy, or inducing nonlinear processes — such as to generate non-classical states of light. Furthermore, Raman scattering in solid core fibre will cause extra noise in the output optical beam of the CBD circuit [17], which will negate the noise suppression goal.

III. RESULTS

A. Implementation in Hollow-Core Fibre

To avoid the nonlinear effects of conventional fibre, we use hollow core fibre (HCF) that guides light predominantly in an air-filled core. Here we used recently-developed free-boundary (or anti-resonant) HCF which has a simple cladding structure comprising of a single ring of silica capillaries fused to a fibre jacket (inset of Fig. 2). The fibre guides light along the core via resonant trapping through the capillary structures [18]. Hence, low-loss guidance along the fibre can be achieved across broad wavelength ranges [19, 20]. The fundamental mode propagates in a large core with almost no overlap with the glass to minimise nonlinearity and dispersion (see Figre 2), while careful control of the capillary dimensions during fabrication enables higher-order modes to be suppressed yet bend loss in the fundamental mode remain manageable [21]. This simple structure enables fabrication of hundreds of metres of fibre with consistent properties and high damage threshold [22].

Hollow core fibre fabrication was by the stack-and-draw process, forming a fibre of six capillaries with an average diameter of 33 μm surrounding a 45 μm core. The fibre had an outer diameter of 160 μm and the thickness of the capillary walls are estimated to be 520 nm. The attenuation of the fundamental mode in the fibre at a wavelength of 1550 nm was found by a cutback measurement on 34 m of fibre to be approximately 0.07 dB/m. By comparison with lengths of conventional single-mode fibre (SMF-28), dispersion of the HCF was estimated to be 1.5 ps/nm/km, which is 9 % of that for conventional single mode fibre (see Supplementary Material). To minimise bend loss within the HCF, the fibre was laid out on a piece of card in a circle of approximately 60 cm in diameter.

The nonlinearity of the HCF is estimated by measuring self-phase modulation induced nonlinear spectral broadening of pulses after propagation along a 35 m HCF delay using an Anritsu MS9740A optical spectrum analyser. The source of pulsed light is a Pritel FFL laser which emits 2 ps pulses at 1550 nm with peak powers of approxi-

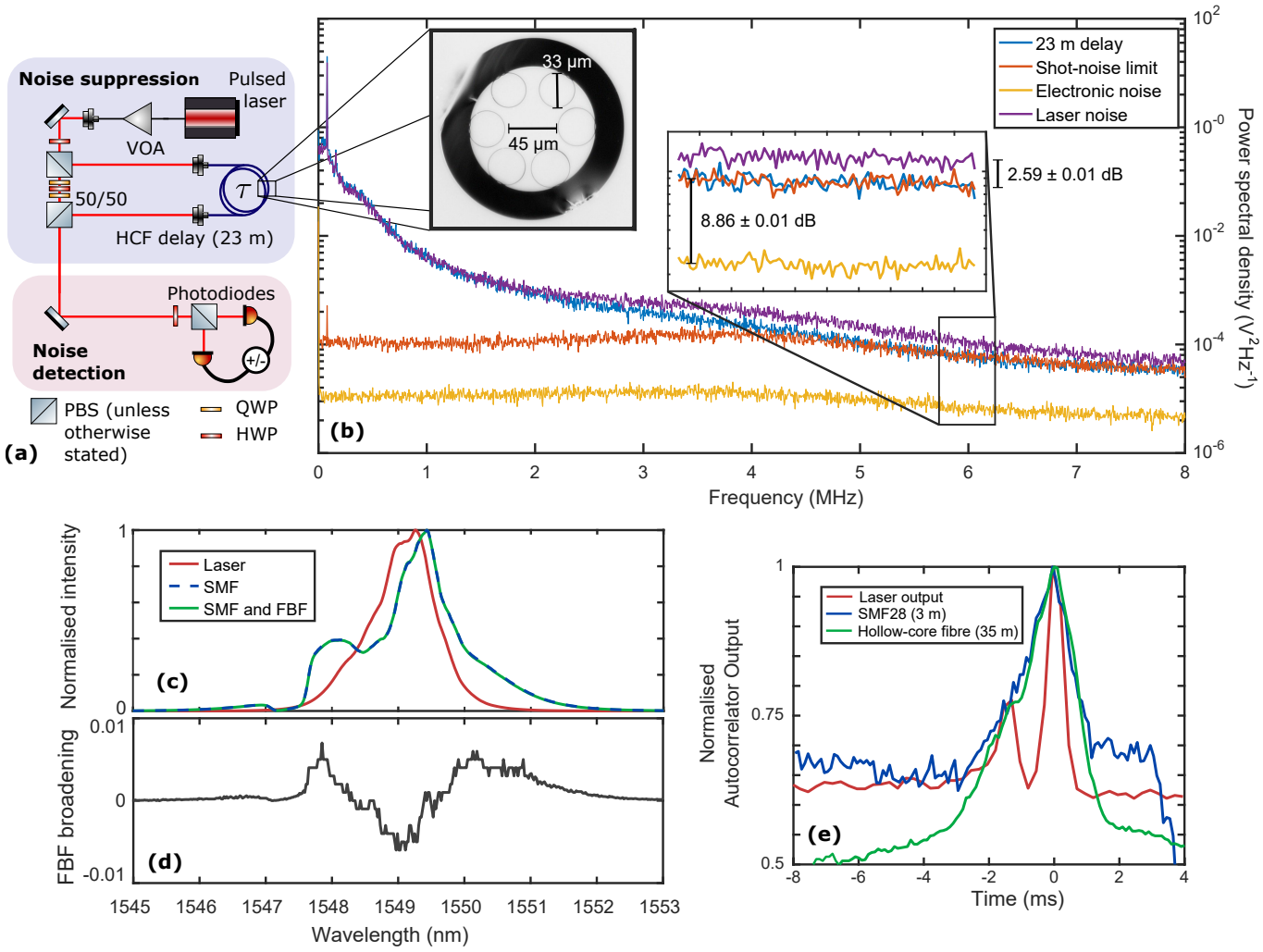

FIG. 2. (a) The optical setup used to construct the asymmetric Mach-Zender interferometer used for noise suppression and the balanced detection technique to measure optical noise. Inset shows the structure of the free-boundary fibre. (b) Measurement results, removing all classical noise at the expected frequency of ~ 6.5 MHz reaching to within 0.011 ± 0.008 dB of the shot-noise limit (averaging the signal in a 0.5 MHz bandwidth centred on 6.5 MHz). Displayed are the noise in the laser without filtering (purple), with filtering (blue), the equivalent power shot-noise limit (red), and electronic noise floor (yellow). The optical nose data here is included in Fig. 4 b), plotted as a noise suppression ration (eq. 1). The common mode rejection ratio for detection in this experiment is > 34 dB and all measurements were performed with a total of 330 μW incident on the balanced detector. (c) The additional spectral broadening induced by the introduction of 35 m of free-boundary fibre (FBF) into the experiment compared with that induced by < 1 m of SMF28. (d) The percentage change in spectrum induced by the FBF, demonstrating that it causes less than a 1% change when compared when it is not present. (e) Comparison of the temporal dispersion introduced by a length of hollow-core free-boundary fibre. The dispersion is comparible with the dispersion introduced by 3 m of SMF28. Colour online.

mately 200 W. In order to couple into the HCF, the pulses propogate through a small (< 1 m) length of SMF28 fibre. Because of this, comparisons are made between propagation through both the SMF28 fibre and HCF, and then bypassing the HCF and only propagating along the SMF28. Figure 2(c) demonstrates that for pulses of this power, the HCF adds negligible amounts of spectral broadening, substantially less than the short amount of solid-core single mode fibre. Figure 2(d) demonstrates less than a 1 percent change in the broadening caused by the free boundary fibre for any particular wavelength component.

The HCF dispersion was investigated using a Toptica FemtoFErb 1560 laser. This laser emits pulses with a 58 fs temporal profile which are approximately 70 nm wide in optical spectrum. The effects of dispersion caused by the HCF are shown in Figure 2(e). When compared with conventional SMF28 fibre, the dispersion in 35 m of hollow-core fibre is comparable with the dispersion in 3 m of SMF28 (which has a quoted dispersion of 18 ps/nm/km [23]). As such we can predict that the dispersion in the HCF is approximately an order of magnitude

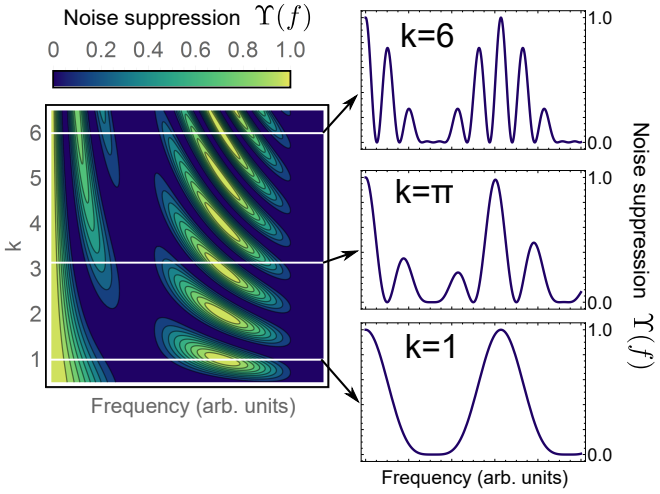

FIG. 3. Theoretical prediction for double-CBD scheme. All plots show the amount of classical noise suppression from two noise suppressing interferometers with delays τ_1 and $\tau_2 = k\tau_1$ respectively. Shown is a contour plot of the predicted noise suppression for arbitrary k, with inset examples for fixed $k = \{6, \pi, 1\}$. Colour online.

less than that expected from refractive index contrast fibres (1.5 ps/nm/km).

We first constructed the CBD circuit in Fig. 2 (a) with a 23 m HCF delay. A half-waveplate and polarising beamsplitter replaces each balanced beamsplitter to fine tune the splitting ratio to compensate for any unbalanced loss in the delay path. Detection of the amplitude noise and shot-noise of the laser light was performed using self-homodyne [17, 24], where the incident light is split on a balanced beamsplitter and detected by two identical photodiodes (Thorlabs FGA01FC with custom amplification circuits). The signals from each photodiode are first filtered via DC (Mini-Circuits BLK-89-S+) and low-pass (Mini-Circuits BLP-21.4+) electronic filters and are then sent to individual channels on a Keysight InfiniiVision MSOX3104A oscilloscope (operated at 2.5 GSa/s). The low-pass filters remove high-frequency noise from the detectors allowing for a higher resolution measurement of the optical noise at the frequencies of interest. The DC filter allows for comparisons of noise at different incident powers to be made without concern for the offset change on the oscilloscope signal. All data captures are taken with a time resolution of 20 μs and with maximum voltage resolution possible for the amplitude of signal (typically 5 - 10 mV/division). The signals are logged on a desktop PC, digitally added or subtracted from one another, and then Fourier transformed to the frequency domain to allow comparison of particular Fourier components of the noise. Subtraction of the photocurrents provides a shot-noise reference for the incident power and addition of the photocurrents provides the noise present in the incoming laser light.

Light from the laser is first attenuated by a digital VOA (Oz Optics DA-100) to attenuate the optical power to work within the range of the detection system, before being launched into free space. The light is split into each path of the AMZI using a half-waveplate and polarising beamsplitter. Waveplates in the non-delayed path match the polarisation of the two paths. The pulse trains are recombined on a second (non-polarising) beamsplitter and the noise characteristics measured. The output of the SMF-28 fibre from the pulsed fibre laser is coupled into free space via a 3-axis stage system (Elliot Scientific) with an aspheric lens system (f = 3.1 mm, Thorlabs C330TMD-C). Coupling into the HCF used an identical system but with a $f = 11.0$ mm (Thorlabs C220TMD-C) lens to allow for mode matching into the large core.

The laser used is an erbium-doped silica fibre laser that is passively mode-locked with a fibre coupled output and generates 2 ps pulses centred at wavelength 1550 nm with a repetition rate of 50 MHz (Pritel FFL). Without operation of the CBD circuit, our laser exhibits super-Poissonian amplitude noise present at all frequencies within the detector bandwidth (0 - 10 MHz). This is shown in Fig. 2 (b) — the raw laser light (purple) contains noise contributions that are larger than the shot-noise limit (red). The laser's raw noise was measured by blocking one of the paths of the interferometer and then reducing the attenuation of the variable optical attenuator (VOA) to keep the power incident on the detectors the same in both suppressed and non-suppressed configurations. The total loss in the delay path is 3.6 ± 0.2 dB, of which approximately 1 dB is from coupling in and out of the HCF and 1.6 dB from propagation loss. With the HCF-CBD circuit in operation, amplitude noise is suppressed as shown in Fig. 2 (b) (blue), reaching to within 0.011 ± 0.008 dB of the shot-noise limit at 6.5 MHz, as predicted for the length of fibre used.

B. Large Bandwidth Suppression

Next, we address the weakness that the original CBD scheme only filters at odd multiples of $f = 1/2\tau$ [16]. We use the stability of fibre-delay to concatenate CBD circuits in series. As any individual CBD circuit does not add noise at any particular frequency, we find that concatenating two CBD circuits, each with delays τ_1 and τ_2, noise suppression follows

$$\Upsilon(f) = \frac{1}{4}(1 + \cos[\pi f \tau_1])(1 + \cos[\pi f \tau_2]). \qquad (2)$$

The theoretical noise suppression across a fixed band of frequencies is shown in Fig. 3.

The average noise reduction across any period of frequencies for a single delay is $\langle \Upsilon(f) \rangle_1 = \frac{1}{2}$, since integrating $0.5(1 + \cos(x))$ (Eq. 1) over a period of the function gives the value of a half. To investigate what the average noise reduction is for a double delay scheme, we consider the subset of cases where $\tau_2 = k\tau_1$ with k taking only integer values. This simplifies the analysis since

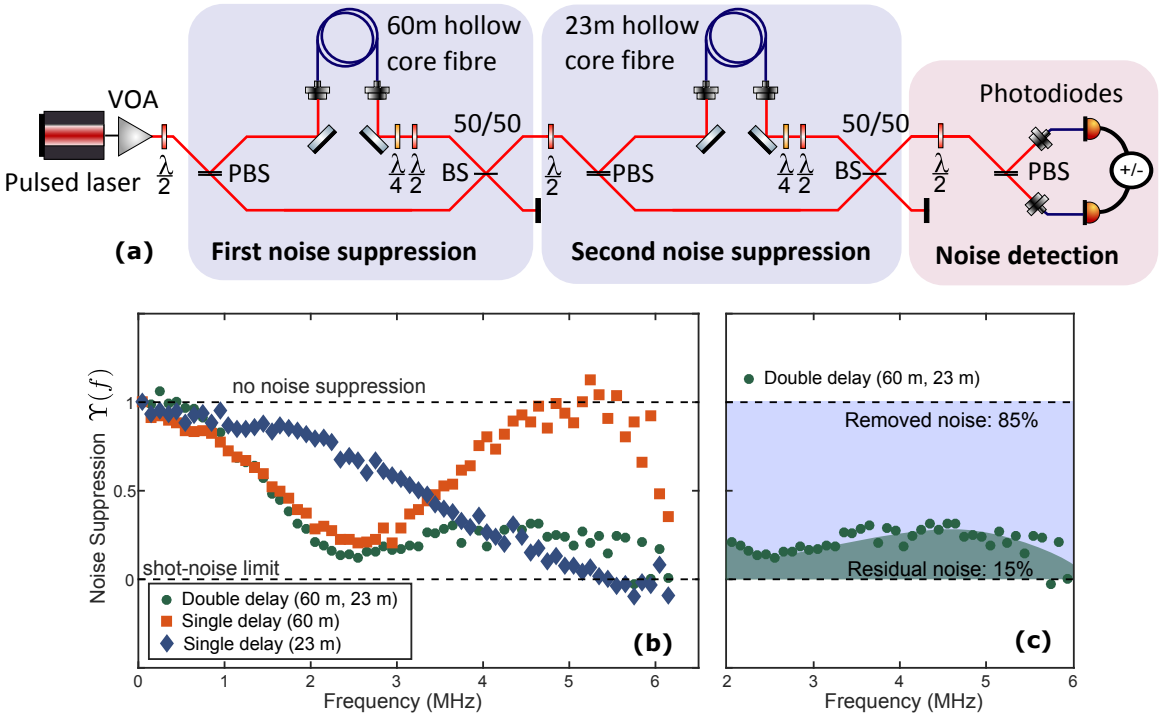

FIG. 4. (a) Experimental setup of two sequential CBD circuits. Each interferometer is constructed as per Fig. 2, but with now two lengths of 60 m and 23 m used as the delays. (b) Experimental results of the performance the double-CBD circuit, for the single delay of 23 m (blue), single delay of 60 m (orange) and both delays (green) in operation in the setup. We note the 60 m single delay suppresses noise at a frequency that is almost one order of magnitude lower than previous demonstrations [14, 15]. The 23 m single delay data is re-plotted from Fig. 2 b). (c) Repeat plot of experimental results for double-CDB circuit from (b), plotted between 2 - 6 MHz illustrating the 85% total noise reduction achieve across this bandwidth. Colour online.

the function $0.25(1+\cos(x))(1+\cos(kx))$ (Eq. 2), for integer k, always has a period between 0 and 2π that we can integrate over to calculate the average noise reduction. The average noise reduction for two delays $\langle\Upsilon(f)\rangle_2$ is equal to

$$\langle\Upsilon(f)\rangle_2 = \frac{1}{2\pi}\int_0^{2\pi}\frac{1}{4}(1+\cos(x))(1+\cos(kx))dx$$
$$= \frac{1}{8\pi}\left[\frac{2k^2-1}{(k^2-1)k}\sin(2\pi k)+2\pi\right].$$

For integer k only, $\sin(2\pi k)=0\ \forall k$, and so the average noise suppression simplifies to $\langle\Upsilon(f)\rangle_2 = 0.25$ for $k \geq 2$. For $k=1$ and number of terms simultaneously tend to zero and so we find that

$$\lim_{k\to 1}\frac{2k^2-1}{(k^2-1)k}\sin(2\pi k) = \pi, \qquad (3)$$

and thus for $k=1$: $\langle\Upsilon(f)\rangle_2 = 3/8 = 0.375$. Therefore we find that for all integer values of k the average noise reduction takes the value of 0.25 apart from the unique value at $k=1$ (interferometers with delays of the same length) where the average noise reduction is reduced to 0.375 of the original value. Non-integer values of k result in an integral range not covering an entire period of the functions in frequency space. Numerical analysis, where the integral range is tuned to always cover an entire period of the function for any rational value of k, indicates that the average noise reduction across a period is always 0.25 apart from the unique value at $k=1$. Note that values of k that are irrational produce aperiodic functions.

To explore this for instances of τ_1 and τ_2, we built the setup in Fig. 4 (a). Fig. 4 (b) displays the experimentally measured values of $\Upsilon(f)$, using a half-wave plate and polarising beamsplitter as tuneable beamsplitters to switch between only one of each CBD circuit suppressing noise and both circuits suppressing noise simultaneously. The total noise suppression across the 2 - 6 MHz bandwidth for the double-CBD scheme is 85% of the original laser noise, which is shown in Fig. 4 (c). For an equivalent bandwidth, the 23 m and 60 m single-CBD implementations each remove less noise as expected: 55% and 41% respectively.

IV. CONCLUSION

These demonstrations show free-boundary HCF can be used to implement CBD to suppress amplitude noise from a fibre laser at MHz frequencies. The cost of each CBD circuit is loss of half of the average power and three quarters of the peak power — the same as passive temporal

multiplexing used to increase laser repetition rate [25]. This suggests use where an overhead in power exists and the need for low amplitude noise takes priority, for example in ultra-sensitive imaging [16, 26–28] and squeezing experiments [29]. While solid core fibre introduces the practicality of a waveguided optical delay, the detrimental nonlinear effects that it has on laser pulses prohibit its use in CBD. Instead, the low optical nonlinearity of air-guiding safeguards spectral and temporal properties of output laser pulses, whilst providing the practicality and stability of a waveguide to further enables concatenation of sequential CBD circuits to suppress amplitude noise at multiple frequencies. Further improvement of the HCF will allow longer delay to be used to suppress at sub-MHz frequencies — iterative design of the fibre structure could reduce propagation loss and lower nonlinearity and dispersion, or create anomalous regimes where soliton formation is possible [30]. Efficient interface between solid core fibre and HCF will be needed for fully-integrated noise suppression, and this has been shown to be possible with as little as 0.3 dB splice loss [31]. Generalisation of CBD itself to continuous-wave light and temporal overlap of the pulses within the interferometer will further widen application and is the subject of future study.

ACKNOWLEDGEMENTS

We are grateful to for assistance on detector electronics Yu Shiozawa. This work was supported by EPSRC programme grant EP/L024020/1, EPSRC UK Quantum Technology Hub in Quantum Enhanced Imaging (EP/M01326X/1), US Army Research Office (ARO) grant no. W911NF-14-1-0133, the EPSRC UK Quantum Technology Hub in Networked Quantum Information Technologies (EP/M013243/1), Innovate UK project FEMTO-AAD (102671), the Australian Research Council (ARC) under the Centre of Excellence for Quantum Computation and Communication Technology (CE170100012), and the Centre for Nanoscience and Quantum Information (NSQI). EA was supported by the Bristol Quantum Engineering Centre for Doctoral Training, EPSRC Grant No. EP/L015730/1. JCFM acknowledges support from an EPSRC Early Careers Fellowship (EP/M024385/1) and an ERC starting grant ERC-2018-STG 803665.

[1] Ibrahim Levent Budunoğlu, Coşkun Ülgüdür, Bulent Oktem, and Fatih Ömer Ilday, "Intensity noise of mode-locked fiber lasers," Opt. Lett. **34**, 2516–2518 (2009).

[2] Nathan R. Newbury and William C. Swann, "Low-noise fiber-laser frequency combs (invited)," J. Opt. Soc. Am. B **24**, 1756–1770 (2007).

[3] R. Paschotta, "Noise of mode-locked lasers (part i): numerical model," Applied Physics B **79**, 153–162 (2004).

[4] WenJun Yue, YunXiang Wang, Cai-Dong Xiong, Zhi-Yong Wang, and Qi Qiu, "Intensity noise of erbium-doped fiber laser based on full quantum theory," J. Opt. Soc. Am. B **30**, 275–281 (2013).

[5] Steve Sanders, Namkyoo Park, Jay W. Dawson, and Kerry J. Vahala, "Reduction of the intensity noise from an erbium-doped fiber laser to the standard quantum limit by intracavity spectral filtering," Applied Physics Letters **61**, 1889–1891 (1992), https://doi.org/10.1063/1.108379.

[6] O. Solgaard and K. Y. Lau, "Optical feedback stabilization of the intensity oscillations in ultrahigh-frequency passively modelocked monolithic quantum-well lasers," IEEE Photonics Technology Letters **5**, 1264–1267 (1993).

[7] R. Lang and K. Kobayashi, "External optical feedback effects on semiconductor injection laser properties," IEEE Journal of Quantum Electronics **16**, 347–355 (1980).

[8] J. Alnis, A. Matveev, N. Kolachevsky, Th. Udem, and T. W. Hänsch, "Subhertz linewidth diode lasers by stabilization to vibrationally and thermally compensated ultralow-expansion glass fabry-pérot cavities," Phys. Rev. A **77**, 053809 (2008).

[9] N. A. Robertson, S. Hoggan, J. B. Mangan, and J. Hough, "Intensity stabilisation of an argon laser using an electro-optic modulator - performance and limitations," Applied Physics B **39**, 149–153 (1986).

[10] M. W. Hamilton, "An introduction to stabilized lasers," Contemporary Physics **30**, 21–33 (1989), https://doi.org/10.1080/00107518908222588.

[11] Hans-Albert Bachor and Timothy C. Ralph, *A guide to experiments in quantum optics* (Wiley, 2004).

[12] Matthew S. Taubman, Howard Wiseman, David E. McClelland, and Hans-A. Bachor, "Intensity feedback effects on quantum-limited noise," J. Opt. Soc. Am. B **12**, 1792–1800 (1995).

[13] David M. Sonnenfroh, W. Terry Rawlins, Mark G. Allen, Claire Gmachl, Federico Capasso, Albert L. Hutchinson, Deborah L. Sivco, James N. Baillargeon, and Alfred Y. Cho, "Application of balanced detection to absorption measurements of trace gases with room-temperature, quasi-cw quantum-cascade lasers," Appl. Opt. **40**, 812–820 (2001).

[14] Keisuke Nose, Yasuyuki Ozeki, Tatsuya Kishi, Kazuhiko Sumimura, Norihiko Nishizawa, Kiichi Fukui, Yasuo Kanematsu, and Kazuyoshi Itoh, "Sensitivity enhancement of fiber-laser-based stimulated raman scattering microscopy by collinear balanced detection technique," Opt. Express **20**, 13958–13965 (2012).

[15] Shota Sawai, Hikaru Kawauchi, Kenichi Hirosawa, and Fumihiko Kannari, "Photon-number squeezing with a noisy femtosecond fiber laser amplifier source using a collinear balanced detection technique," Opt. Express **21**, 25099–25106 (2013).

[16] Christian W. Freudiger, Wenlong Yang, Gary R. Holtom, Nasser Peyghambarian, Sunney X. Xie, and Khanh Q. Kieu, "Stimulated raman scattering microscopy with a robust fibre laser source," Nature Photonics **8**, 153 (2014).

[17] S. Schmitt *et al.*, "Photon-number squeezed solitons from an asymmetric fiber-optic sagnac interferometer," Phys.

Rev. Lett. **81**, 2446–2449 (1998).

[18] N. M. Litchinitser, A. K. Abeeluck, C. Headley, and B. J. Eggleton, "Antiresonant reflecting photonic crystal optical waveguides," Optics Letters **27**, 1592–1594 (2002).

[19] David Bird, "Attenuation of model hollow-core, antiresonant fibres," Optics Express **25**, 23215–23237 (2017).

[20] Fei Yu, William J. Wadsworth, and Jonathan C. Knight, "Low loss silica hollow core fibers for 3–4 μm spectral region," Opt. Express **20**, 11153–11158 (2012).

[21] Walter Belardi and Jonathan C. Knight, "Hollow antiresonant fibers with low bending loss," Optics Express **22**, 10091–10096 (2014).

[22] Piotr Jaworski, Fei Yu, Robert R.J. Maier, William J. Wadsworth, Jonathan C. Knight, Jonathan D. Shephard, and Duncan P. Hand, "Picosecond and nanosecond pulse delivery through a hollow-core negative curvature fiber for micro-machining applications," Opt. Express **21**, 22742–22753 (2013).

[23] "Thorlabs," `https://www.thorlabs.de/navigation.cfm`, accessed: 2018-05-23.

[24] Ulrich Busk Hoffn, *Integrated Quantum Optics: Experiments towards integrate quantum-light sources and quantum-enhanced sensing*, Ph.D. thesis, Department of Physics, Technical University of Denmark (2007).

[25] M. A. Broome, M. P. Almeida, A. Fedrizzi, and A. G. White, "Reducing multi-photon rates in pulsed down-conversion by temporal multiplexing," Opt. Express **19**, 22698–22708 (2011).

[26] Michael A. Taylor and Warwick P. Bowen, "Quantum metrology and its application in biology," Physics Reports **615**, 1–59 (2016).

[27] Alessio Gambetta, Vikas Kumar, Giulia Grancini, Dario Polli, Roberta Ramponi, Giulio Cerullo, and Marco Marangoni, "Fiber-format stimulated-raman-scattering microscopy from a single laser oscillator," Optics Letters **35**, 226–228 (2010).

[28] Jaime Ortega Arroyo and Philipp Kukura, "Non-fluorescent schemes for single-molecule detection, imaging and spectroscopy," Nature Photonics **10**, 11 (2016).

[29] U. L. Andersen, T. Gerhing, C. Marquardt, and G. Leuchs, "30 years of squeezed light generation," Physica Scripta **91**, 053001 (2016).

[30] Jonathan C. Knight, "Photonic crystal fibres," Nature **424**, 847 (2003).

[31] R. Thapa, K. Knabe, K. L. Corwin, and B. R. Washburn, "Arc fusion splicing of hollow-core photonic bandgap fibers for gas-filled fiber cells," Opt. Express **14**, 9576–9583 (2006).